AD-A207 522 THE QUANTITATIVE DEPENDENCE OF TRANSMISSIVITY ON 1/1
FLEXURAL STRAIN FOR MULT (U) ARMY LAB COMMAND
WATERTOWN MA MATERIAL TECHNOLOGY LAB J A KIDD FEB 89
UNCLASSIFIED MTL-TR-89-14 F/G 20/6.1 NL

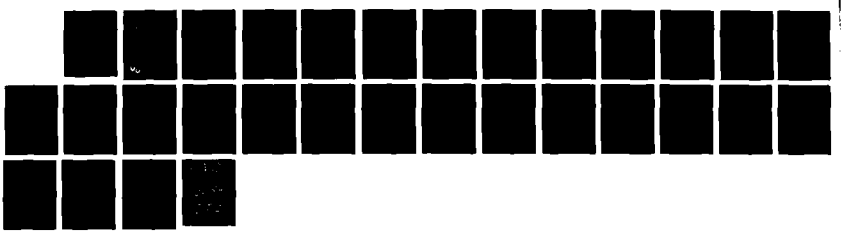

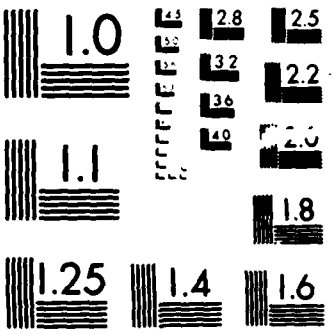

MICROCOPY RESOLUTION TEST CHART

MTL TR 89-14

AD

THE QUANTITATIVE DEPENDENCE OF TRANSMISSIVITY ON FLEXURAL STRAIN FOR MULTIMODE OPTICAL FIBER

JAMES A. KIDD, Jr.
MATERIALS TESTING & EVALUATION BRANCH

February 1989

Approved for public release; distribution unlimited.

US ARMY
LABORATORY COMMAND
MATERIALS TECHNOLOGY LABORATORY

U.S. ARMY MATERIALS TECHNOLOGY LABORATORY
Watertown, Massachusetts 02172-0001

The findings in this report are not to be construed as an official Department of the Army position, unless so designated by other authorized documents.

Mention of any trade names or manufacturers in this report shall not be construed as advertising nor as an official indorsement or approval of such products or companies by the United States Government.

DISPOSITION INSTRUCTIONS

Destroy this report when it is no longer needed.
Do not return it to the originator.

UNCLASSIFIED

SECURITY CLASSIFICATION OF THIS PAGE (When Data Entered)

REPORT DOCUMENTATION PAGE		READ INSTRUCTIONS BEFORE COMPLETING FORM
1 REPORT NUMBER MTL TR 89-14	2 GOVT ACCESSION NO	3 RECIPIENT'S CATALOG NUMBER
4 TITLE (and Subtitle) THE QUANTITATIVE DEPENDENCE OF TRANSMISSIVITY ON FLEXURAL STRAIN FOR MULTIMODE OPTICAL FIBER		5 TYPE OF REPORT & PERIOD COVERED Final Report 6 PERFORMING ORG. REPORT NUMBER
7 AUTHOR(s) James A. Kidd, Jr.		8 CONTRACT OR GRANT NUMBER(s)
9 PERFORMING ORGANIZATION NAME AND ADDRESS U.S. Army Materials Technology Laboratory Watertown, Massachusetts 02172-0001 SLCMT-MRM		10 PROGRAM ELEMENT, PROJECT, TASK AREA & WORK UNIT NUMBERS AMCMS Code No. 53970M6350
11 CONTROLLING OFFICE NAME AND ADDRESS U.S. Army Laboratory Command 2800 Powder Mill Road Adelphi, Maryland 20783-1145		12 REPORT DATE February 1989 13 NUMBER OF PAGES 24
14 MONITORING AGENCY NAME & ADDRESS (If different from Controlling Office)		15 SECURITY CLASS. (of this report) Unclassified 15a DECLASSIFICATION/DOWNGRADING SCHEDULE

16 DISTRIBUTION STATEMENT (of this Report)

Approved for public release; distribution unlimited.

17 DISTRIBUTION STATEMENT (of the abstract entered in Block 20, if different from Report)

18 SUPPLEMENTARY NOTES

Presented at ASTM Symposium on Factors that Affect the Precision of Mechanical Tests; Bal Harbour, Florida.

(See Reverse)

19 KEY WORDS (Continue on reverse side if necessary and identify by block number)

Optical fibers
Fiber optics
Attenuation
Transmission loss
Macrobending
Transmissivity
Strain (mechanics)

20 ABSTRACT (Continue on reverse side if necessary and identify by block number)

(SEE REVERSE SIDE)

DD FORM 1 JAN 73 1473 EDITION OF 1 NOV 65 IS OBSOLETE

UNCLASSIFIED

SECURITY CLASSIFICATION OF THIS PAGE (When Data Entered)

Block No. 18

This project has been accomplished as part of the U.S. Army Materials Testing Technology Program, which has for its objective the timely establishment of testing techniques, procedures or prototype equipment (in mechanical, chemical, or nondestructive testing) to insure efficient inspection methods for materiel/material procured or maintained by AMC.

Block No. 20

ABSTRACT

Four different multimode optical fibers were tested to obtain the following correlations: 1) signal power with bend radius, 2) strain with bend radius, and 3) signal power with strain. The data are presented numerically, graphically, and mathematically. Graded index multimode and step index multimode fibers are discussed. The mechanism for the attenuation of light in optical fiber as a result of macrobending is examined. Three of the tested fibers demonstrated a consistent relationship between flexural strain and light transmissivity and could potentially be inlaid within a curved composite material system for use as the principal component in a stress or strain transducer.

CONTENTS

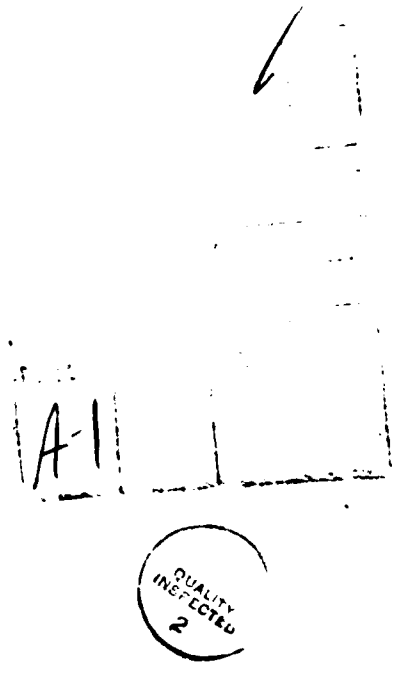

INTRODUCTION

In the middle of the eighteen hundreds, an Irish physicist named John Tyndall conducted an experiment in which he placed a mirror at an angle in a bucket of water such that the mirror reflected sunlight into a stream of water which flowed through an orifice near the bottom of the bucket. After the light entered the stream, it followed the curvilinear path of the water demonstrating that light can be guided by means of successive reflections within a medium of high refractive index (water) which is surrounded by a medium with a lower refractive index (air). The same principle of total internal reflection is the foundation of all optical fibers.[1]

Optical fibers can be employed in many highly diversified applications. Optical fiber technology has been used extensively in telecommunications, the medical field, and for weapon system guidance and control. Generally, manufacturers of optical fiber strive to minimize the light loss characteristics of their product for most environmental conditions. However, loss of light from an optical fiber which is subjected to specific types of stress can be useful if the fiber is used as the sensory element in a transducer.

This work demonstrates that the flexural strain of a deflected optical fiber can be inferred from measuring variations in light intensity passing through the fiber; the affect of uniaxial elongation with uniform cross-sectional strain was not investigated.

THEORY

Two types of optical fibers were examined: graded index multimode and step index multimode. Graded index fibers have a core in which the index of refraction (speed of light in a vacuum, $C = 3(10)^5$ Km/sec, divided by the speed of light at a specific point in the core) decreases toward the circumference of the core. The core is enclosed within a homogeneous cladding. The light follows a quasi-sinusoidal path with turning points that depend on the angle of incidence (angle between an incident ray and a line which is perpendicular to the longitudinal axis of the fiber) and the index profile, n(x). The profile of the refractive index in the core of a graded index fiber is usually parabolic and is a function of the radius:

$$n(x) = n_1 \sqrt{1 - \left[\frac{(n_1)^2 - (n_2)^2}{(n_1)^2}\right]\left(\frac{x}{j}\right)^g}$$

where

- n_1 = the axial (central) refractive index of the core
- n_2 = refractive index at the outer edge of the core (same as that of homogeneous cladding)
- x = radial coordinate of the point for which n(x) is being calculated
- j = maximal radius of the core
- g = profile parameter, characterizes the distribution of the fiber's refractive index [when g = 2, the fiber has a square law profile (parabolic)].[2]

For example, if $n_1 = 1.48$, $n_2 = 1.46$, $j = 25\,\mu m$, $g = 2$, and we want n(x) at $x = 0.5j$, or at $x = 12.5\,\mu m$, then:

$$n(x) = 1.48 \sqrt{1 - \left(\frac{1.48^2 - 1.46^2}{1.48^2}\right)\left(\frac{12.5\,\mu m}{25\,\mu m}\right)^2} = 1.475 \quad .$$

1. LEWIS, K. H. *Principles and Applications of Fiber-Optic Communication Systems.* Lightech, Inc., Richardson, Texas, 1986, p. 2-2.
2. BOCKO, P. L., and GANNON, J. R. *Optical Waveguide Materials.* Corning Glass Works, Corning, New York, August 1983, p. 1 and 2.

Because the velocity of light in the core, v = C/n, increases as the path approaches the cladding and decreases as it approaches the centerline of the core, the speed of light compensates for the various path lengths so that all modes (paths) emerge from the fiber at essentially the same time.

Step index fibers have a homogeneous core with a constant refractive index surrounded by a homogeneous cladding with a lower refractive index. The light follows a zigzag path with angular turning points.

Macrobending losses occur when the bend radius of the fiber decreases to the point that photons* of light escape into the cladding. For a light mode to maintain its integrity when traversing a bend, the outer portion of the mode must travel a greater distance and travel faster than the inside portion of the mode. If the bend radius becomes sharp enough, eventually the outer portion of the mode must travel faster than C to avoid loss; because this is impossible, some light travels into the cladding which attenuates the amount of transmitted light. The phenomenon of total internal reflection of light within the core of a step index fiber ceases when the angle of incidence, θ_i, is reduced to less than the critical angle, θ_c:

$$\theta_c = \text{Arcsin}\left(\frac{n_{\text{cladding}}}{n_{\text{core}}}\right).$$

For a fixed bend radius, the probability of $\theta_i < \theta_c$, when light leaves the core and enters the cladding, generally increases as the wavelength of light increases.[3,†] Typically, optical fiber operates using radiation with a fixed wavelength: 800 nm $\leq \lambda \leq$ 1,600 nm;[4] this range is within the infrared section, 780 nm to 100,000 nm, of the electromagnetic spectrum.[5] Because the light emitting diode used for this work produced radiant energy at a single wavelength of 900 nm, the affect of wavelength on the transmissivity of deflected optical fiber was not examined.

DESCRIPTION OF SPECIMENS, EQUIPMENT, AND TEST FIXTURE

Four different types of optical fibers were tested. The specimens were 61 cm (24 in.) long and were terminated with male SMA ferrules (cylindrical electro-optical connectors). The specifications for each of the specimens are in Table 1. The column labeled $\frac{a}{b}$ provides the actual ratio between the cross-sectional area of the core and that of the cladding. The column labeled $\frac{a}{a+b}$ lists what is commonly called the "core to cladding ratio."

Table 1. CROSS-SECTIONAL SPECIFICATIONS OF TESTED OPTICAL FIBER

Type of Fiber	Diameter of Core, micrometers (mils)	Outside Diameter of Cladding, micrometers (mils)	Outside Diameter of Acrylic Buffer, micrometers (mils)	$\frac{a}{b}$ *	$\frac{a}{a+b}$ *
Graded Index, Multimode	50 (1.97)	125 (4.92)	218 (8.60)	0.19	0.16
Graded Index, Multimode	63 (2.48)	125 (4.92)	142 (5.60)	0.34	0.25
Step Index, Multimode	80 (3.15)	100 (3.94)	100 (3.94) No Buffer	1.78	0.64
Step Index, Multimode	100 (3.94)	140 (5.51)	285 (11.2)	1.04	0.51

*"a" equals the area of the core; "b" equals the area of the cladding

*See Appendix A.

†Personal communication with Otto I. Szentesi, Siecor Corporation, Hickory, North Carolina.

3 LEWIS, K. H. *Principles and Applications of Fiber-Optic Communication Systems.* Lightech, Inc., Richardson, Texas, 1986, p. 4-30.

4 LEWIS, K. H. *Principles and Applications of Fiber-Optic Communication Systems.* Lightech, Inc., Richardson, Texas, 1986, p. 4-27.

5 JAY, F. ed., *IEEE Standard Dictionary of Electrical and Electronics Terms.* Second Edition, (IEEE Std 100-1977), The Institute of Electrical and Electronics Engineers, Inc., New York, New York, 1977, p. 331.

The following commercial equipment was used:

1. Optical power source (transmitter)
2. Light Emitting Diode (LED) source, 900 nm, 2μW minimum, with male AMP ferrule (conical electro-optical connector)
3. Sensor head adaptor for male SMA ferrule
4. Silicon photodiode sensor head (400 to 1,150 nm)
5. Light power meter (receiver)
6. Ambient light power meter.

The ambient light power meter measured illuminance, the density of luminous flux on a surface, in SI units of lux (lumens/m^2) and in footcandles (lumens/ft^2). A splice was required to connect the LED source with an AMP ferrule to the SMA ferrules on the optical fiber specimens; the splice was unavailable commercially. The SMA-AMP splice was designed as shown in Figure 1; it was fabricated from polymethyl methacrylate (lucite).

To enhance repeatability of the data, the test fixture shown in Figure 2 was used. The fixture, which was made from lexan (transparent and more resistant to impact damage than lucite), was designed such that for all radii the fixture will hold 50.8 cm (20 in.) of the specimen; this arrangement leaves 5.1 cm (2 in.) at each end of the specimen for attaching instrumentation.

EXPERIMENTAL AND ANALYTICAL PROCEDURES

The subsequent test plan for correlating optical fiber transmissivity with the deflection and with the maximal surface strain of the fiber was followed for each type of fiber:

1. Measure the intensity of the ambient light
2. Monitor output of power source to ensure consistency of light intensity introduced into fiber
3. Measure received signal power versus fifteen bend radii (including radius = ∞ for straight fiber) four times for four different optical fibers and average the results for each bend radius
4. Plot signal power against bend radii; describe the power versus radii curve with two different forms of equations and graphically compare results
5. For each radii, calculate the maximal surface strain of the deflected optical fiber
6. Plot maximal surface strain against bend radii; describe the curve mathematically and compare the results graphically
7. Plot signal power versus maximal surface strain; use linear regression to obtain an equation which represents the correlation
8. If the received signal power is sensitive to ambient light, the affect can be quantified by repeating steps 1 through 7 with the test fixture covered with opaque material.

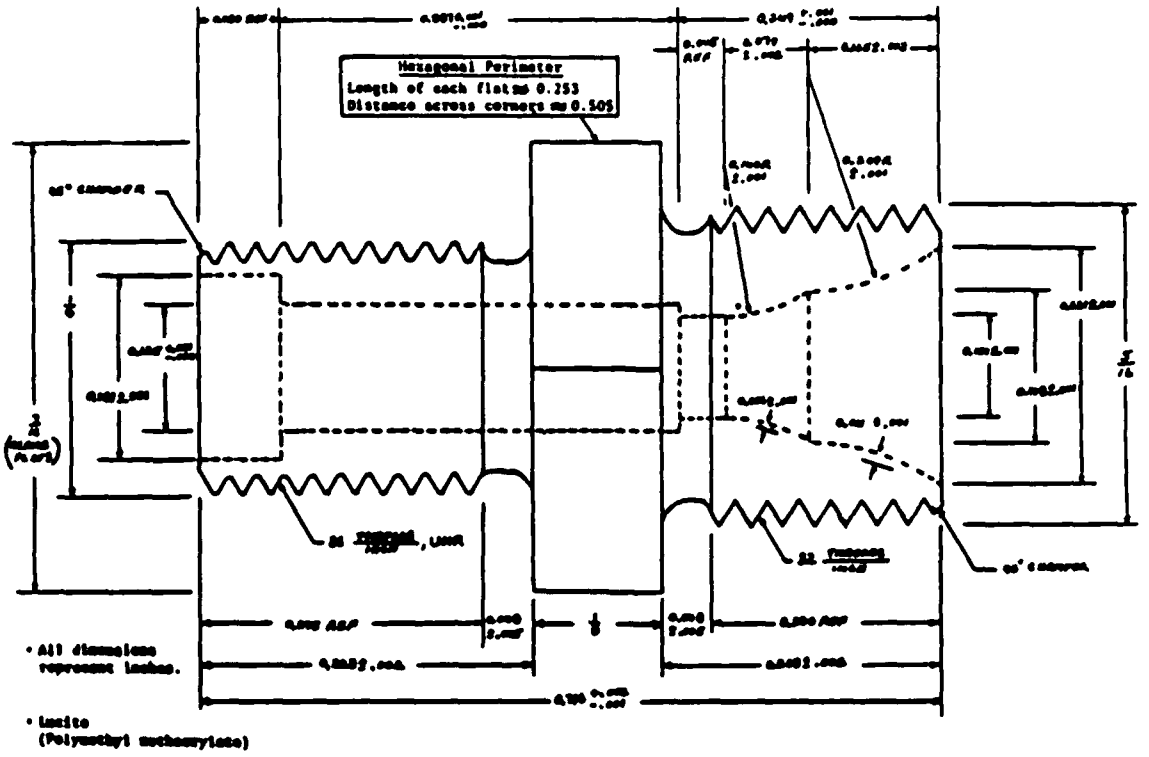

Figure 1. SMA-AMP fiber optic splice.

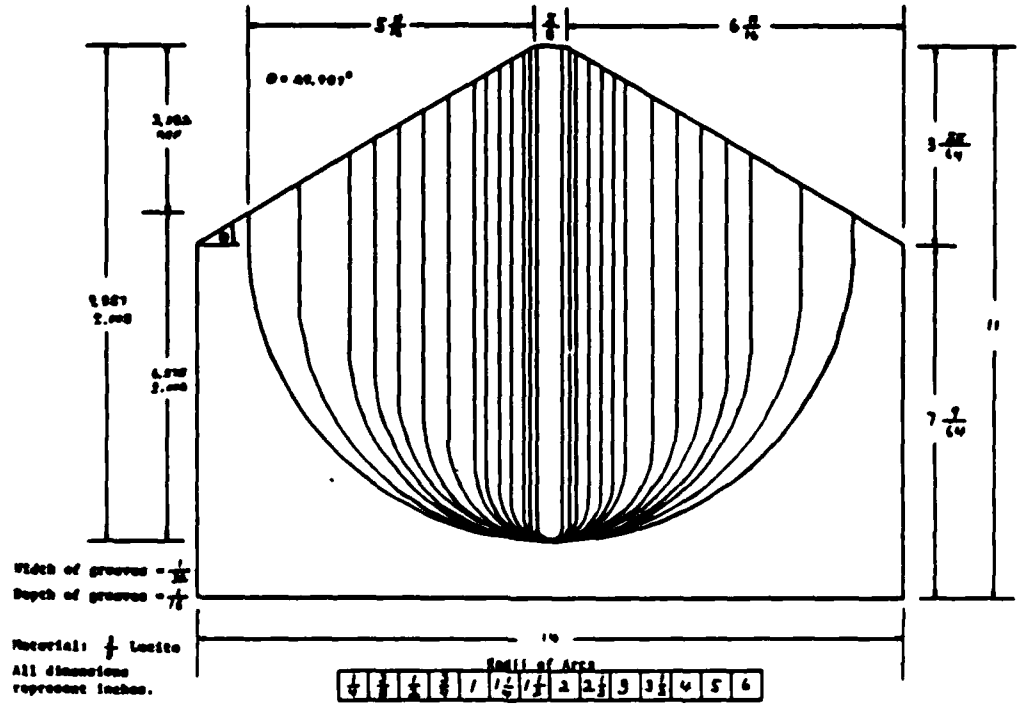

Figure 2. Fiber optic test fixture.

RESULTS

The results from the four types of optical fiber are shown in Table 2. Each value for signal power is the mean of four measurements collected at room temperature and ambient humidity.

Table 2. BEND RADIUS WITH CORRESPONDING MEAN SIGNAL POWER

Bend Radius, cm (in.)	Received Power, nW			
	Graded Index 50/125/218*	Graded Index 63/125/142*	Step Index 80/100/100*	Step Index 100/140/285*
∞	6.44	12.94	6.06	28.05
15.24 (6.00)	6.45	12.87	5.98	27.60
12.70 (5.00)	6.43	12.72	6.00	27.12
10.16 (4.00)	6.41	12.61	5.94	26.75
8.89 (3.50)	6.42	12.59	5.92	26.37
7.62 (3.00)	6.42	12.42	5.88	25.77
6.35 (2.50)	6.36	12.30	5.88	25.45
5.08 (2.00)	6.33	12.15	5.88	24.75
3.81 (1.50)	6.12	11.59	5.86	23.85
3.175 (1.25)	5.93	11.19	5.85	22.22
2.54 (1.00)	5.77	11.03	5.83	21.85
1.905 (0.75)	5.53	10.91	5.81	19.57
1.27 (0.50)	5.10	10.59	5.82	17.72
0.952 (0.375)	4.63	9.57	5.63	15.27
0.635 (0.25)	3.66	8.25	5.83	12.70

*Core/cladding/outside diameter, μm

The intensity of ambient light, from natural and fluorescent sources, reaching the test fixture was varied from essentially 0 lux, covering the test fixture with opaque material, to approximately 37 lux. The ambient light did not have a perceptible affect on the results; therefore, the tests were not repeated with a shield blocking the fixture and specimen from external light.

The maximal change in signal power for each specimen when deflected from a straight line to a bend radius of 0.635 cm (0.25 in.) is:

1. graded index, 50/125: -2.79 nW ➡ - 43.32% or -2.47 dB*
2. graded index, 63/125: -4.69 nW ➡ - 36.24% or -1.95 dB
3. step index, 80/100: insignificant loss
4. step index, 100/140: -15.35 nW ➡ - 54.72% or -3.44 dB.

*See Appendix B.

With the exception of the step index fiber (80/100), all of the tested fibers showed a significant reduction in transmissivity as the bend radius was decreased. Figures 3a, 3b, 3c, and 3d; 4a, 4b, 4c, and 4d; 5a, 5b, 5c, and 5d graphically display the results with the alphabetical designation indicating:

a. plot of experimental data for bend radius versus transmissivity

b. power curve fit of the data, $P_{sig} = wr^{i}$, using the least squares logarithmic method

c. curve fit using $P_{sig} = k\,(s)^{\frac{1}{r}}$

d. composite graph with the empirical data curve and the two curve fits

where

P_{sig} = received signal power, nanowatts

r = bend radius, inches

w, i, and s = constants

k = maximal value of ordinate, value of P_{sig} when $r = \infty$.

The strain in the plane of bending on the surface of a deflected optical fiber is inversely proportional to the bend radius. An expression for maximal flexural surface strain as a function of the bend radius was derived as follows:

1. The length of a 180° circular arc = π (radius of the arc).

2. Strain, $\varepsilon = \frac{\Delta L}{L}$ where ΔL is the change in length; L is the original length.

3. Assume that the cross-sectional area of the deflected fiber remains circular; r is the bend radius from the center of the arc to the longitudinal centerline of the optical fiber; D_o is the outside diameter of the fiber which was measured with a micrometer.

4. For a 180° arc, $\varepsilon = \frac{\Delta L}{L} = \frac{\pi\,(r + 0.5D_o) - \pi r}{\pi r} = \frac{D_o}{2r}$.

It should be noted that this expression represents the surface strain of a fiber on the outside of the arc. The surface strain of a fiber on the inside of the arc is equal in magnitude, but of opposite sign:

$$\varepsilon = \frac{\Delta L}{L} = \frac{\pi\,(r - 0.5D_o) - \pi r}{\pi r} = -\frac{D_o}{2r} \quad .$$

Deflection of an optical fiber induces a cross-sectional strain gradient with positive flexural strain outside of the neutral axis and negative flexural strain inside of the neutral axis; therefore, the average cross-sectional strain is zero.

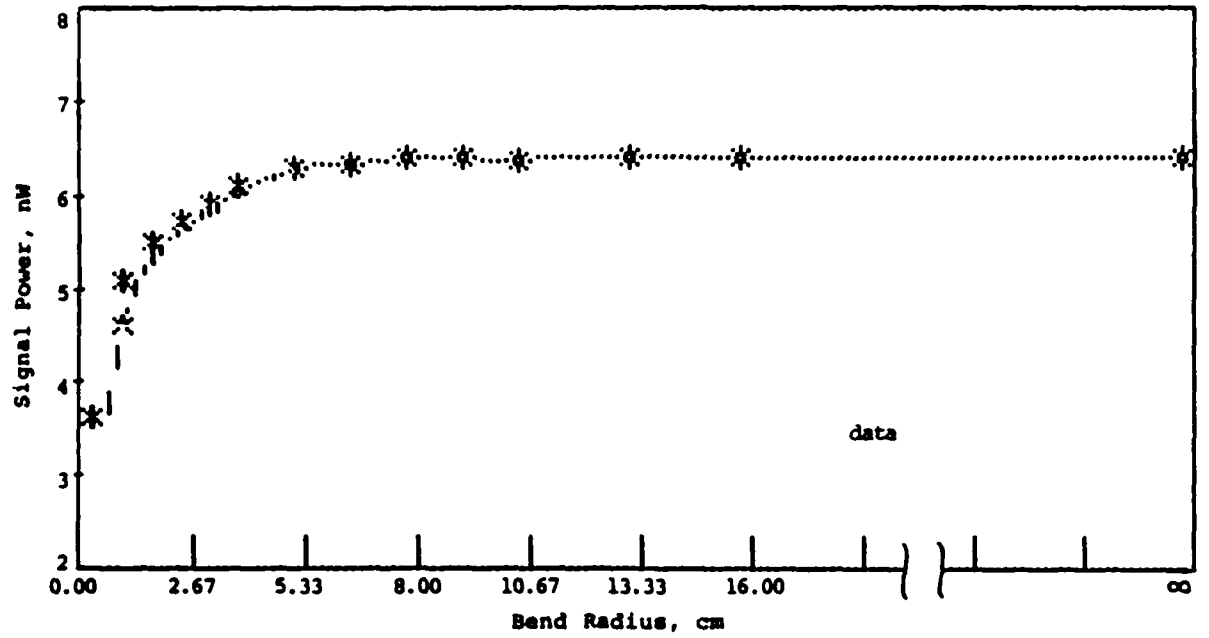

(a)

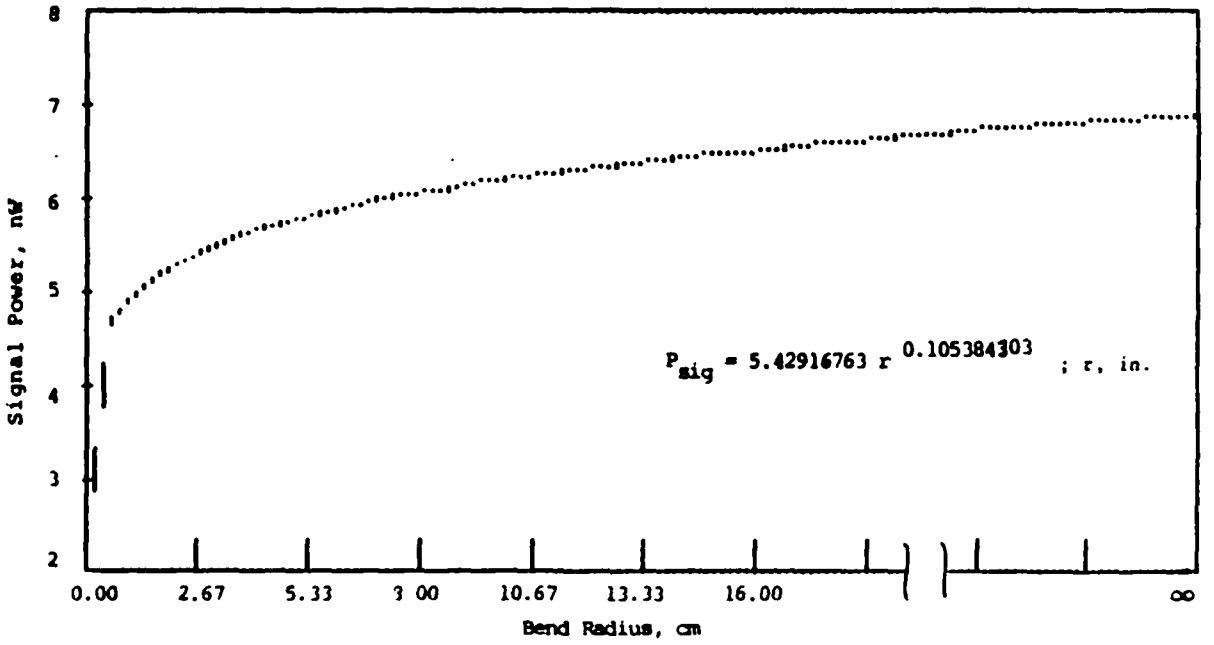

(b)

Figure 3. Transmissivity versus bend radius, 50/125/218 optical fiber.

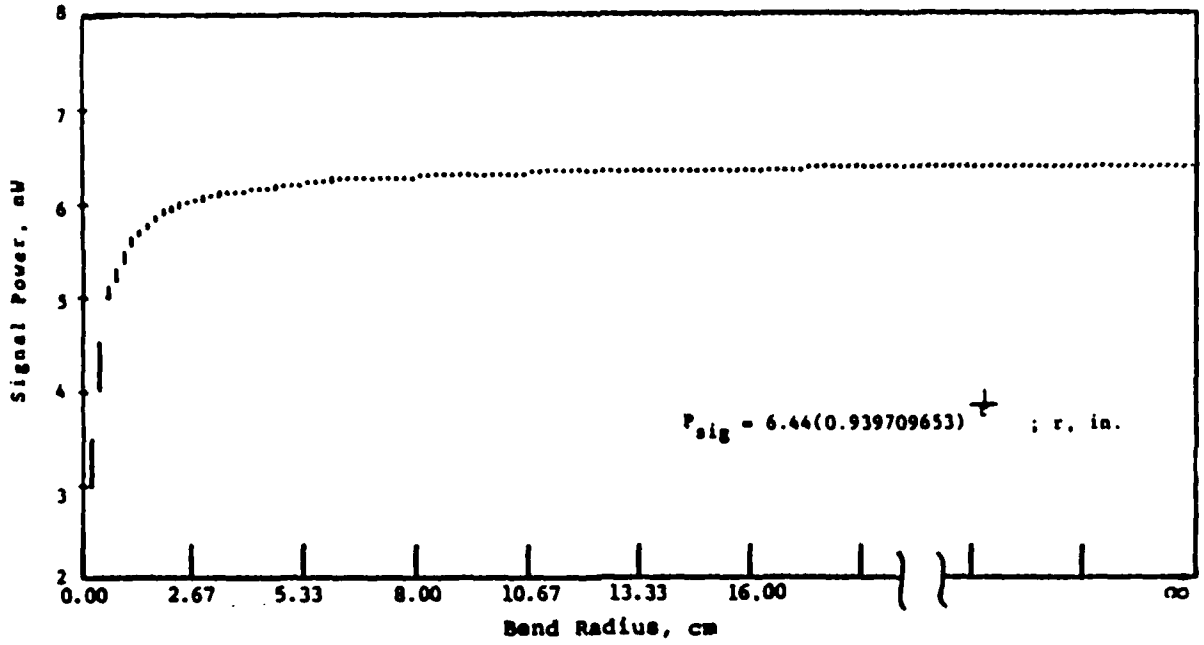

(c)

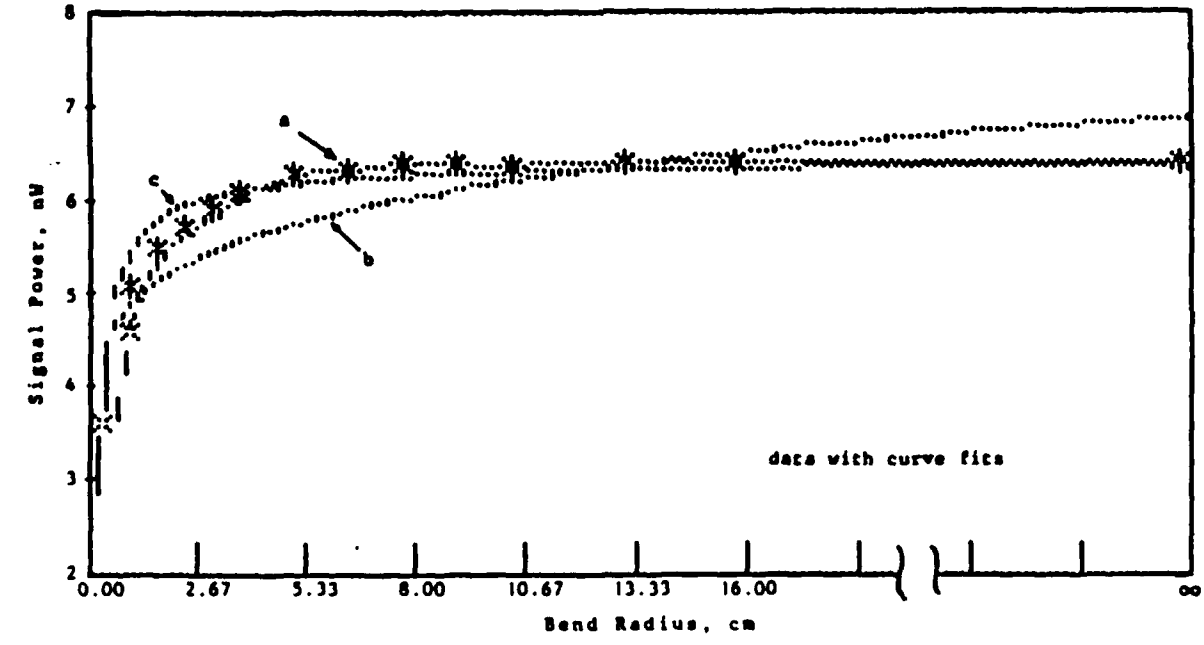

(d)

Figure 3 (Cont'd). Transmissivity versus bend radius, 50/125/218 optical fiber.

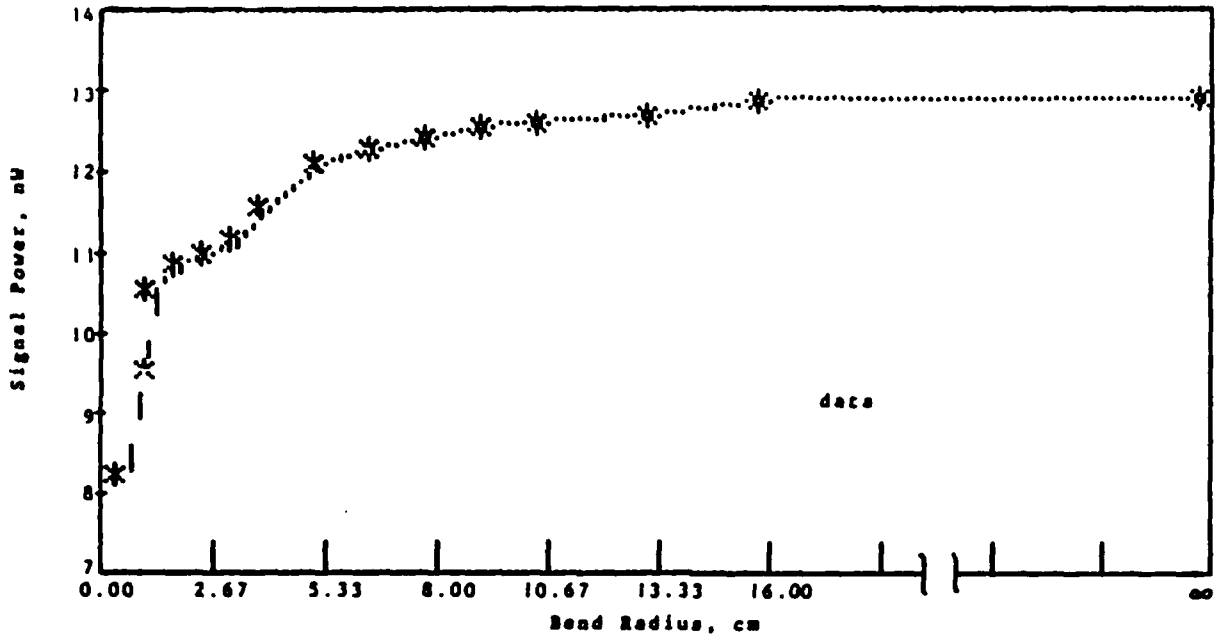

(a)

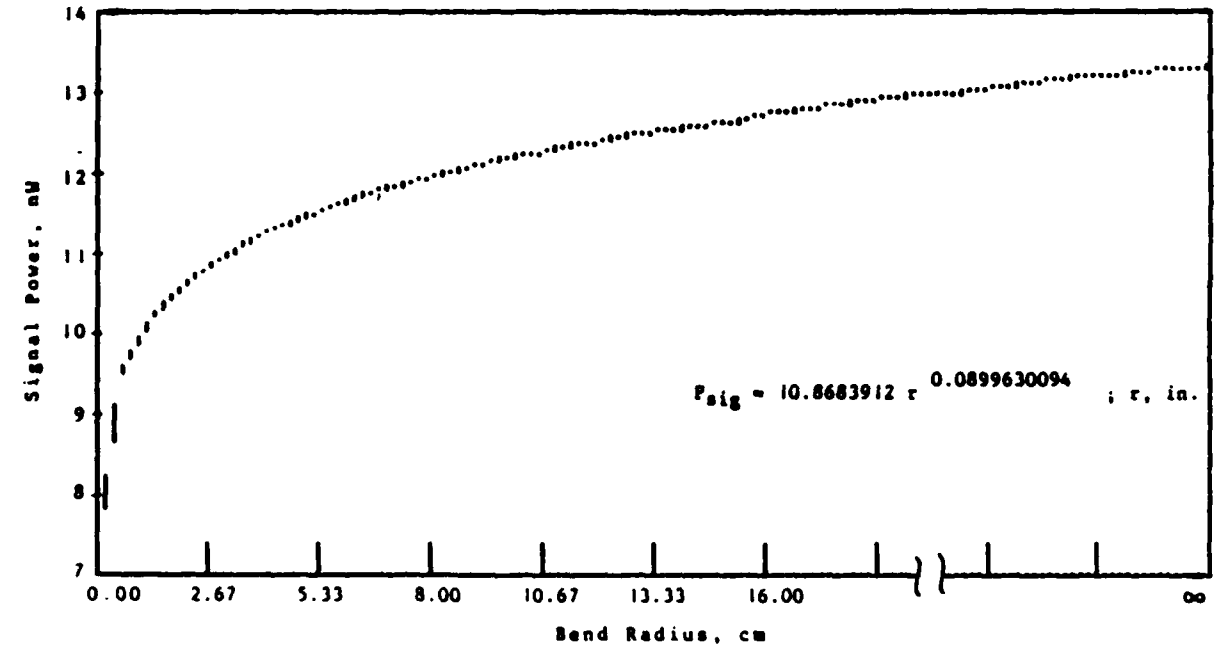

(b)

Figure 4. Transmissivity versus bend radius, 63/125/142 optical fiber.

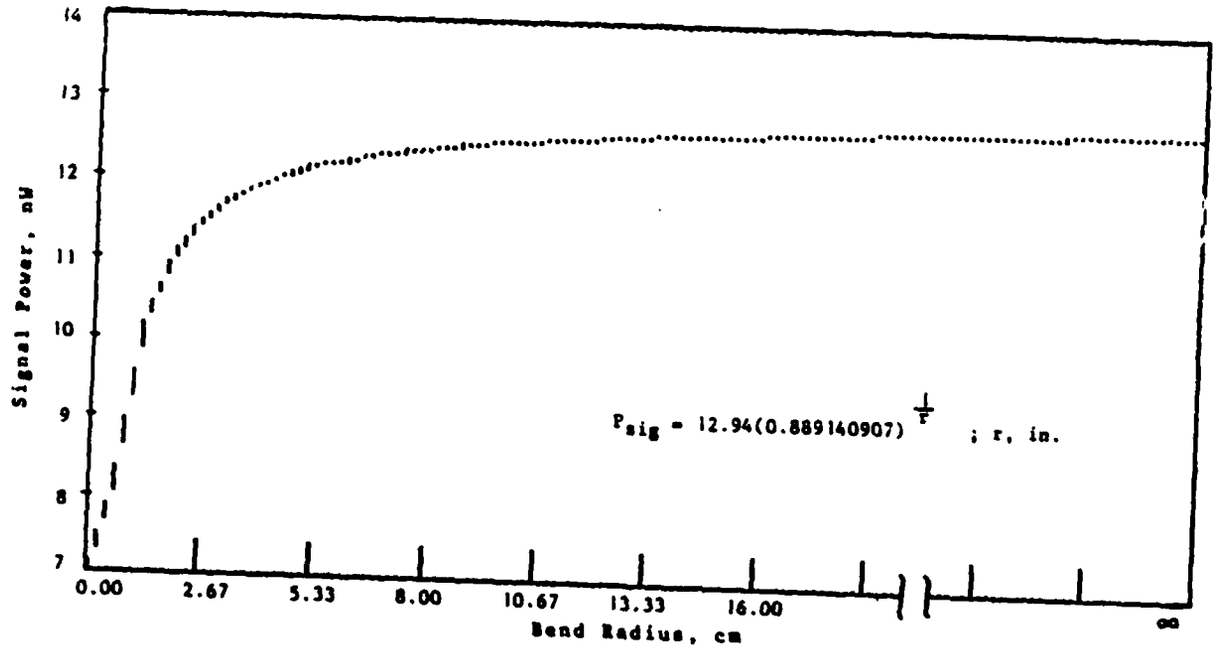

(c)

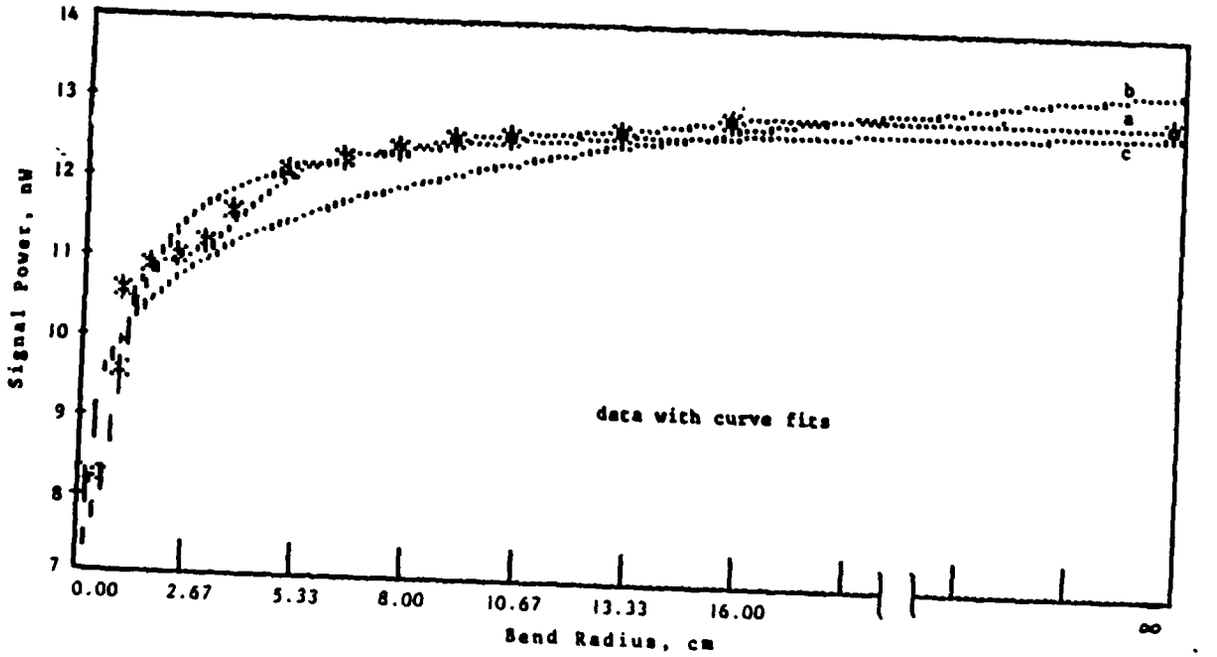

(d)

Figure 4 (Cont'd). Transmissivity versus bend radius, 63/125/142 optical fiber.

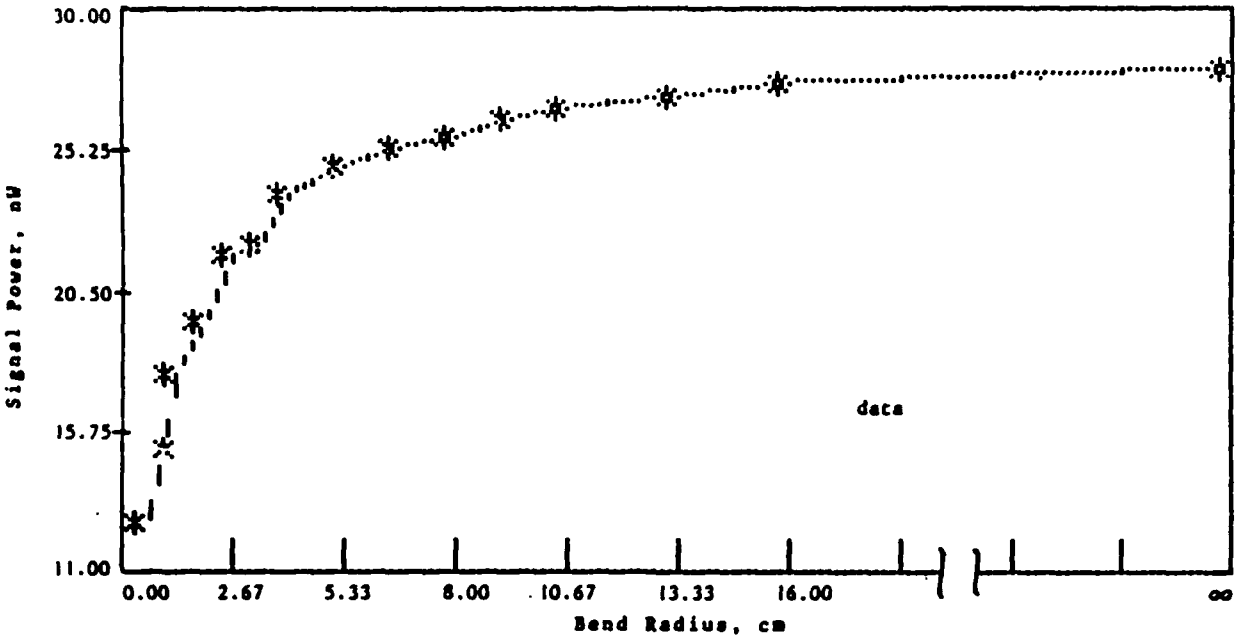

(a)

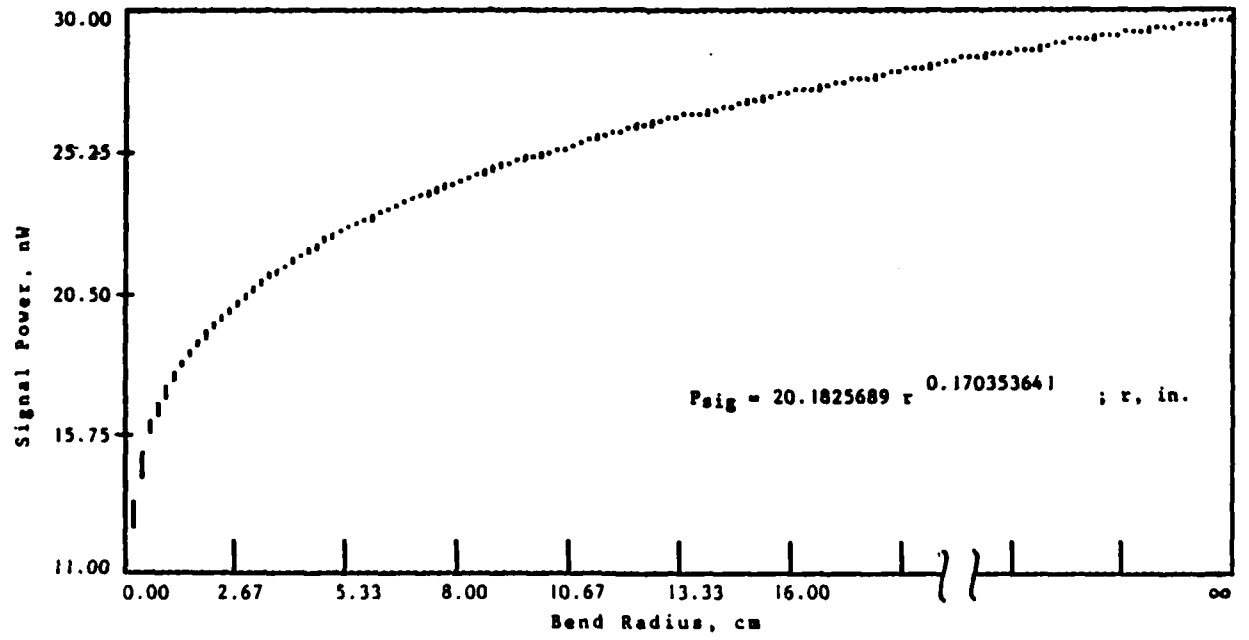

(b)

Figure 5. Transmissivity versus bend radius, 100/140/285 optical fiber.

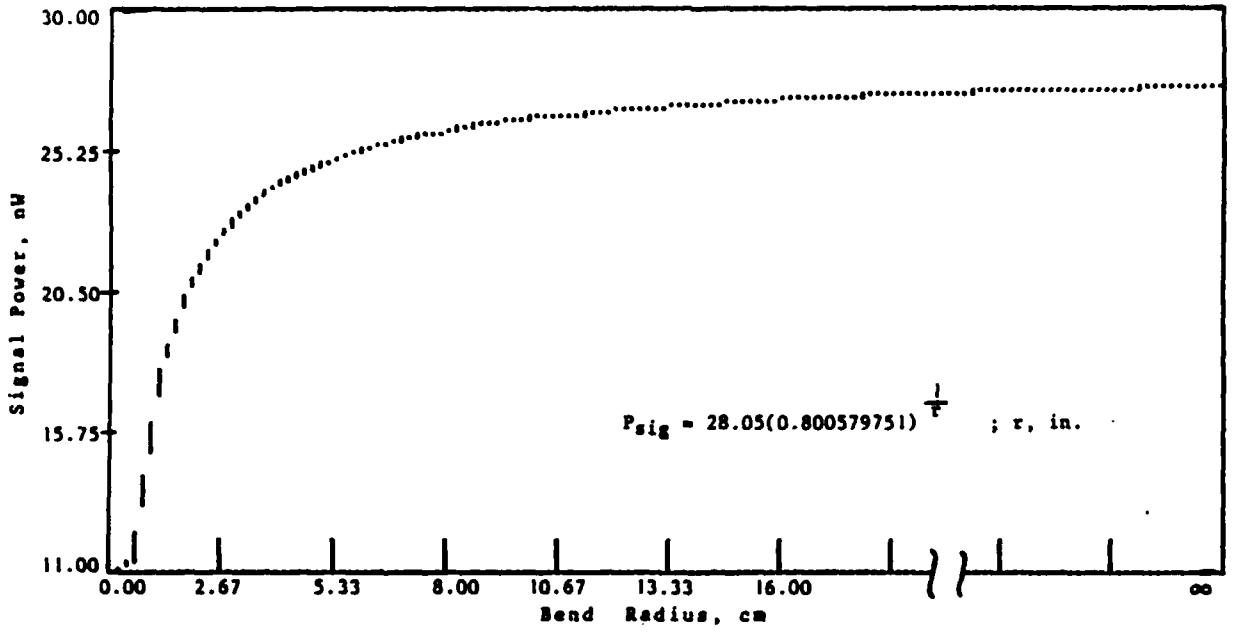

(c)

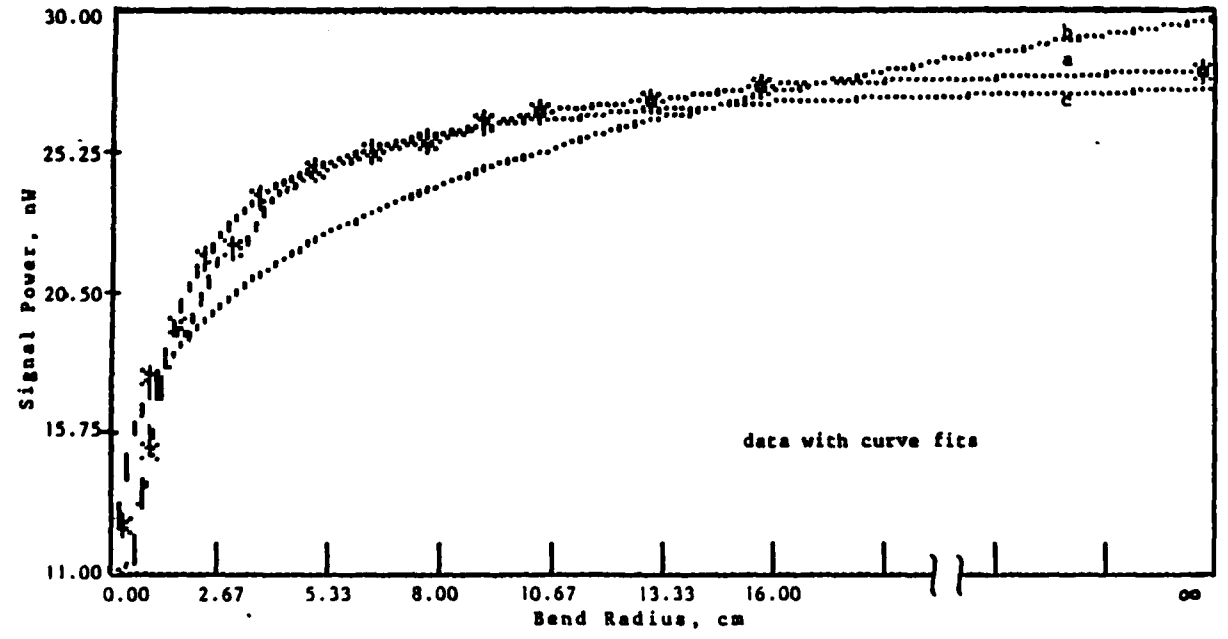

(d)

Figure 5 (Cont'd). Transmissivity versus bend radius, 100/140/285 optical fiber.

The surface strain on the outside arc for the three fibers which displayed a significant loss of transmissivity with a reduction of bend radius is shown in Table 3.

Table 3. FLEXURAL SURFACE STRAIN OF DEFLECTED OPTICAL FIBERS

Bend Radius, cm (in.)	Strain		
	Graded Index 50/125/218*	Graded Index 63/125/142*	Step Index 100/140/285*
∞	0.00000	0.00000	0.00000
15.24 (6.00)	0.00072	0.00047	0.00093
12.70 (5.00)	0.00086	0.00056	0.00112
10.16 (4.00)	0.00108	0.00070	0.00140
8.89 (3.50)	0.00123	0.00080	0.00160
7.62 (3.00)	0.00143	0.00093	0.00187
6.35 (2.50)	0.00172	0.00112	0.00224
5.08 (2.00)	0.00215	0.00140	0.00280
3.81 (1.50)	0.00287	0.00187	0.00373
3.175 (1.25)	0.00344	0.00224	0.00448
2.54 (1.00)	0.00430	0.00280	0.00560
1.905 (0.75)	0.00573	0.00373	0.00747
1.27 (0.50)	0.00860	0.00560	0.01120
0.952 (0.375)	0.01147	0.00747	0.01493
0.635 (0.25)	0.01720	0.01120	0.02240

*Core/cladding/outside diameter, μm

Figures 6a and 6b, 7a and 7b, and 8a and 8b are graphs of the results and graphs of the power curve fits of the calculated data with the corresponding equation in the form $\varepsilon = qr^{-t}$, where $\varepsilon \Rightarrow$ maximal flexural surface strain, $r \Rightarrow$ bend radius in centimeters, and q and t are the coefficient and exponent found by a least squares regression.

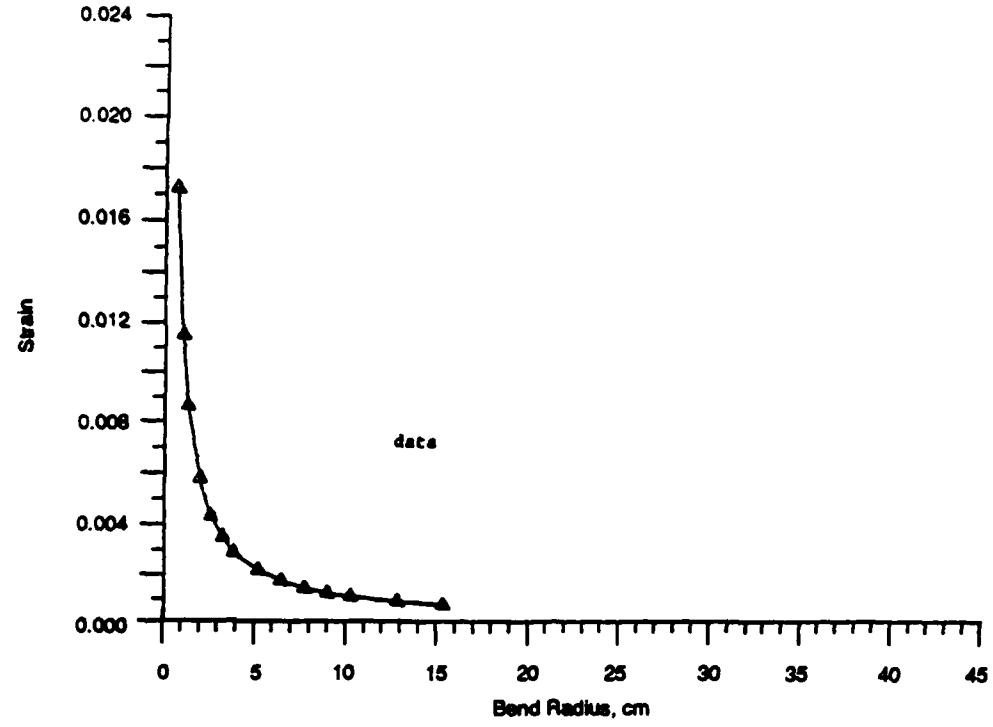

(a)

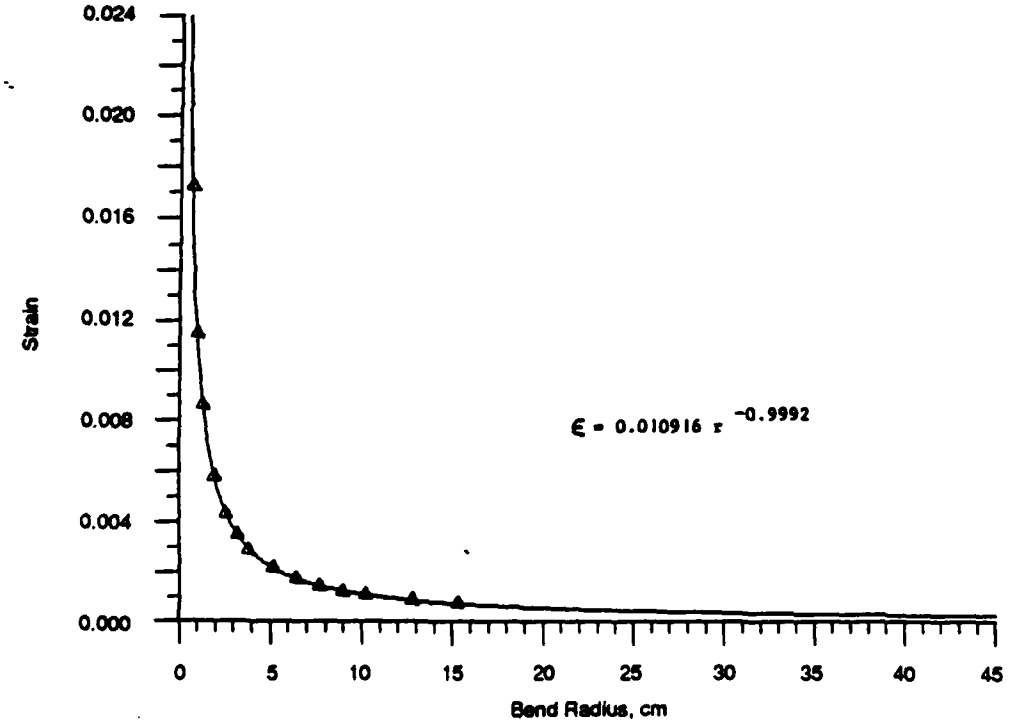

(b)

Figure 6. Flexural surface strain of 50/125/218 optical fiber.

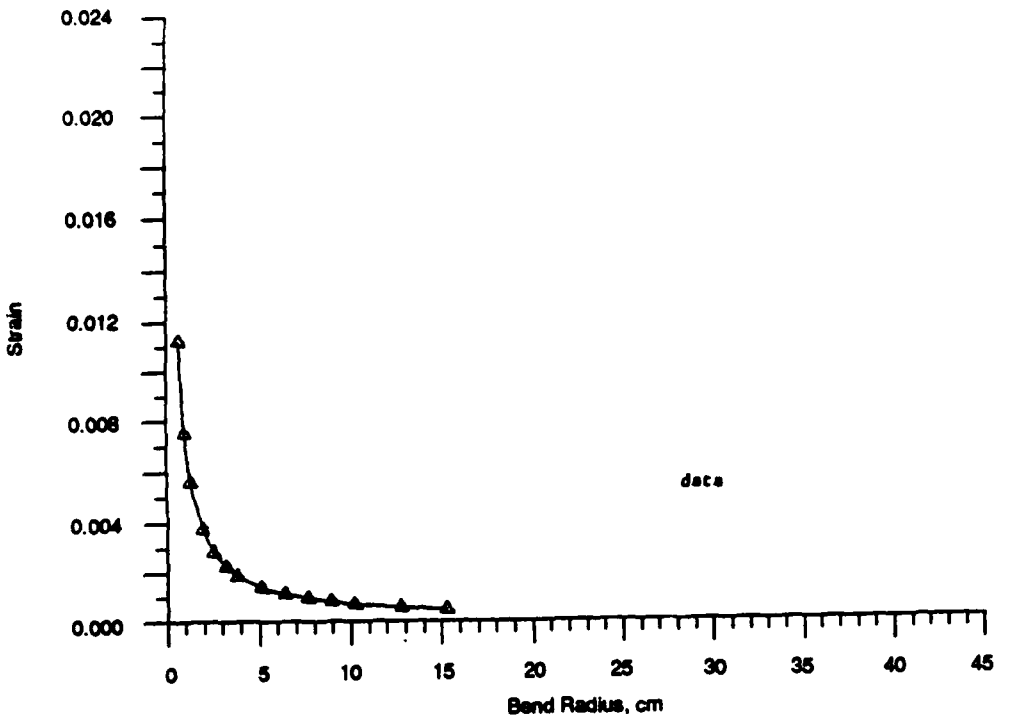

(a)

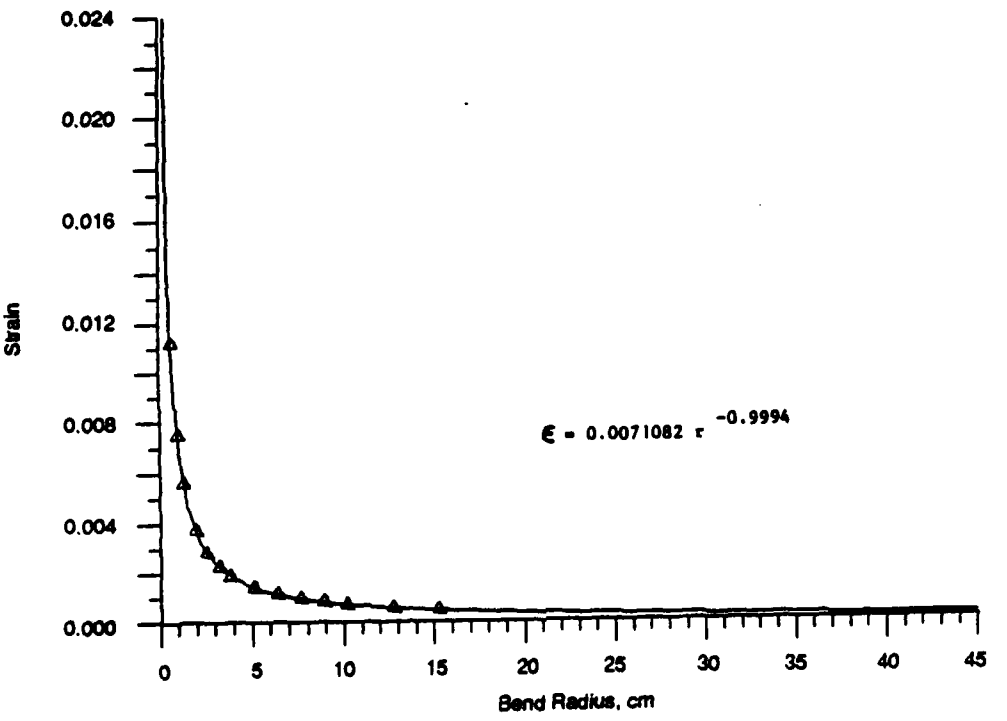

(b)

Figure 7. Flexural surface strain of 63/125/142 optical fiber.

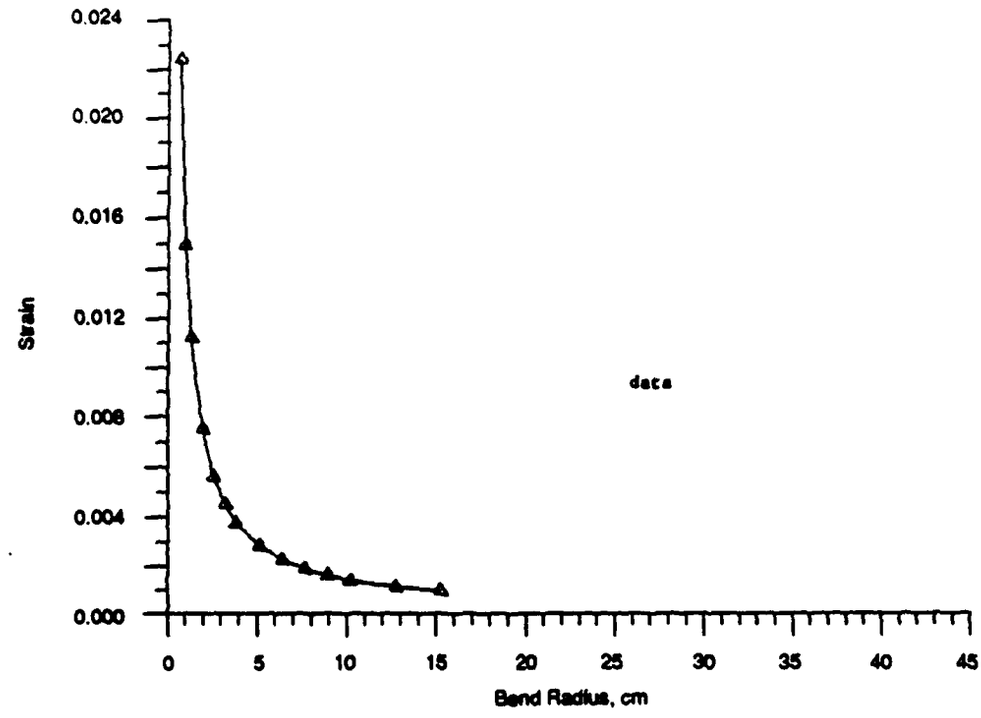

(a)

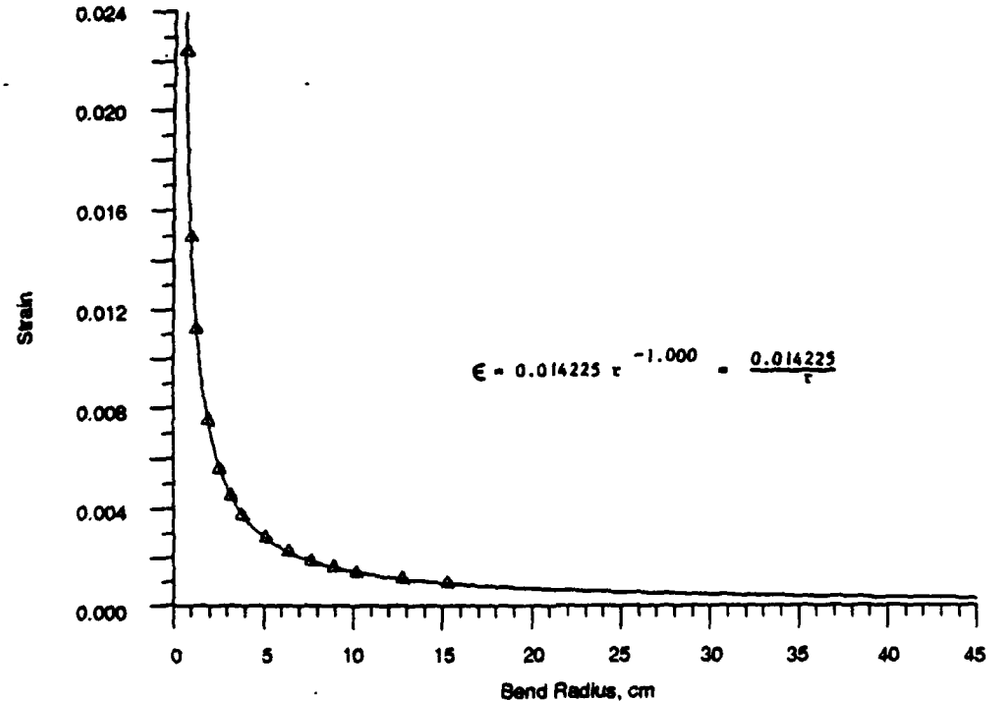

(b)

Figure 8. Flexural surface strain of 100/140/285 optical fiber.

The results in Tables 2 and 3 are combined in Table 4 which provides maximal flexural surface strain with the corresponding signal (received) power.

Table 4. CORRELATION OF OPTICAL FIBER TRANSMISSIVITY WITH FLEXURAL SURFACE STRAIN

Graded Index 50/125/218*		Graded Index 63/125/142*		Step Index 100/140/285*	
Flexural Surface Strain	Received Power, nW	Flexural Surface Strain	Received Power, nW	Flexural Surface Strain	Received Power, nW
0.00000	6.44	0.00000	12.94	0.00000	28.05
0.00072	6.45	0.00047	12.87	0.00093	27.60
0.00086	6.43	0.00056	12.72	0.00112	27.12
0.00108	6.41	0.00070	12.61	0.00140	26.75
0.00123	6.42	0.00080	12.59	0.00160	26.37
0.00143	6.42	0.00093	12.42	0.00187	25.77
0.00172	6.36	0.00112	12.30	0.00224	25.45
0.00215	6.33	0.00140	12.15	0.00280	24.75
0.00287	6.12	0.00187	11.59	0.00373	23.85
0.00344	5.93	0.00224	11.19	0.00448	22.22
0.00430	5.77	0.00280	11.03	0.00560	21.85
0.00573	5.53	0.00373	10.91	0.00747	19.57
0.00860	5.10	0.00560	10.59	0.01120	17.72
0.01147	4.63	0.00747	9.57	0.01493	15.27
0.01720	3.65	0.01120	8.25	0.02240	12.70

*Core/cladding/outside diameter, μm

The data indicate an essentially inverse linear relationship as shown in Figures 9, 10, and 11. These figures are accompanied with a regressive linear equation in the form $P_{sig} = m\varepsilon + B$, where P_{sig} ➡ signal power, ε ➡ maximal flexural surface strain, m ➡ slope, and B ➡ intercept of P_{sig}.

This linear relationship between P_{sig} and ε can be derived by combining two equations, $P_{sig} = wr^i$ and $\varepsilon = qr^{-t}$, as follows:

1. Solving the second equation for r produces:

$$r = \left(\frac{q}{\varepsilon}\right)^{\frac{1}{t}}$$

2. Substituting into $P_{sig} = wr^i$ results in:

$$P_{sig} = w\left[\left(\frac{q}{\varepsilon}\right)^{\frac{1}{t}}\right]^i = w\left(\frac{\varepsilon}{q}\right)^{\frac{i}{t}}$$

3. Assume $t = i$: $\frac{t}{i} = 1$, then $P_{sig} = w\left(\frac{\varepsilon}{q}\right)$

4. Let $\frac{w}{q} = m$ and let B = a constant representing the intercept at the maximal value of P_{sig}

5. Therefore, $P_{sig} = m\varepsilon + B$, the equation of a straight line.

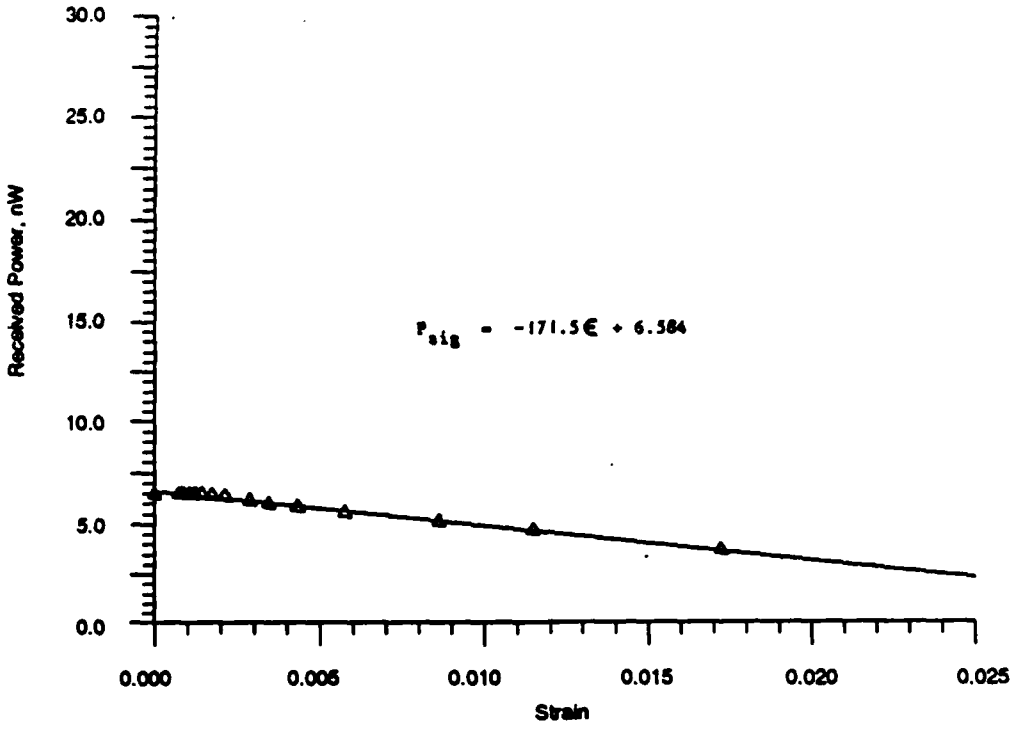

Figure 9. Transmissivity versus strain of 50/125/218 optical fiber.

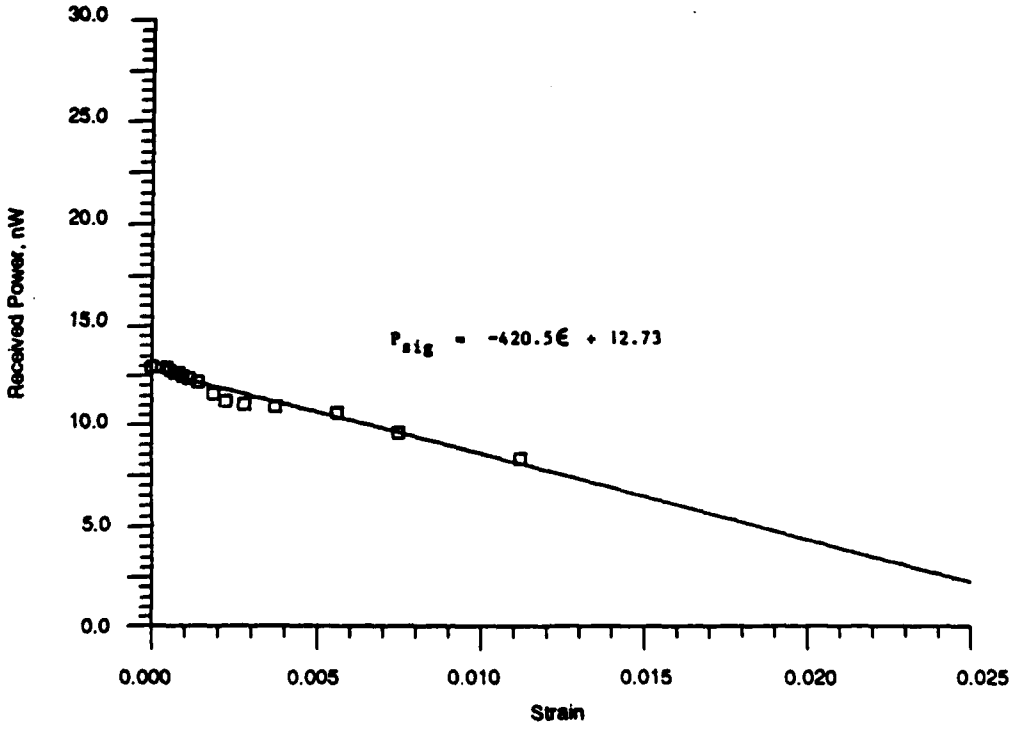

Figure 10. Transmissivity versus strain of 63/125/142 optical fiber.

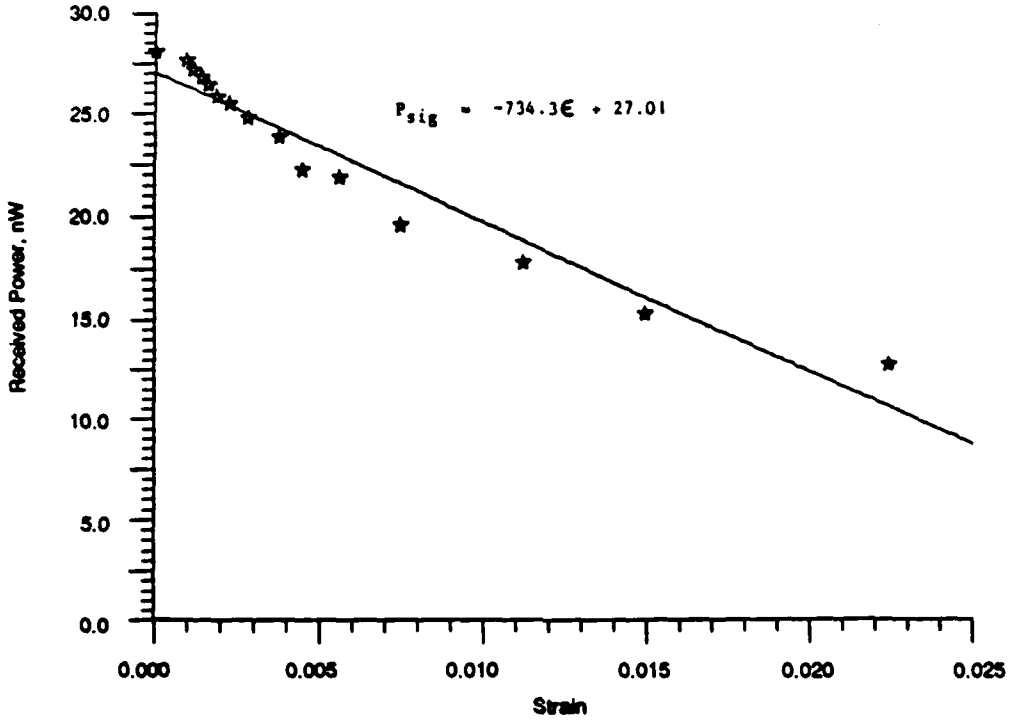

Figure 11. Transmissivity versus strain of 100/140/285 optical fiber.

DISCUSSION AND CONCLUSIONS

Of the four multimode optical fibers, three (two graded index and one step index) produced results which showed a definite correlation between flexural strain and the capability of the fiber to transmit light. The step index fiber without an acrylic buffer did not display this correlation. As indicated in Table 1, this fiber (80 μm core, 100 μm cladding) had the highest areal ratio of core to cladding. The other fibers transmitted light at a level close to an asymptote which was equal to the maximal received signal power which occurred when the fiber was straight; this level did not decrease sharply until the bend radius was decreased to below approximately three to five cm. Ultimately, P_{sig} would be reduced to zero if the fiber was kinked with a bend radius equal to zero. The correlation between signal power and bend radius is described extremely well by the equations used for Figures 3c, 4c, and 5c. Similarly, the maximal flexural surface strain increased markedly when the bend radius was decreased below this same range and was asymptotic to zero strain as the bend radius approached infinity. Combining the results of signal power and bend radius with maximal flexural surface strain and bend radius produces an essentially inverse linear relationship between optical fiber transmissivity and flexural strain. The three fibers which consistently showed a diminution of light transmissivity with increasing flexural strain could possibly be inlaid within a curved (because of inadequate sensitivity when the fiber is only deflected slightly) composite material system for use as the sensor in a stress (the modulus of elasticity for the composite material would be required so that stress could be inferred from deflection of the fiber) or strain transducer.

Future work could involve using wavelength as an independent variable (with various bend radii) to measure its affect on transmissivity. Step index single mode fiber typically have a core diameter of 9 microns or less with a cladding diameter of 125 microns and usually transmit light with a wavelength of 1,300 nm or 1,550 nm. The combination of the small core and longer wavelength could make step index single mode fiber more susceptible to bending loss than step index multimode or graded index multimode fiber. Therefore, an investigation which quantified the sensitivity of step index single mode fiber to flexural strain should produce interesting results.

ACKNOWLEDGMENTS

Authority for this project was granted by Roger M. Lamothe, former Chief of the Materials Properties Branch. Machining of the test fixture and the fiber optic splice was accomplished by Patsy A. Luongo and George N. Vangel, respectively. Wayne M. Bethoney and William L. Crenshaw provided assistance with graphics. Specialized computer programming for this report was performed by Luke J. Rheaume, a former employee of the U.S. Army Materials Technology Laboratory and an employee of Mitre Corporation, Bedford, MA, U.S.A. This research was supported by the U.S. Department of the Army as part of the Materials Testing Technology Program.

APPENDIX A. QUANTIFICATION OF PHOTON ENERGY

A photon or gamma ray is a quantum of electromagnetic radiation with energy $E = hf$, where h is Planck's constant, $6.626(10)^{-34}$ joule-second, and f is the frequency of a specific light, $\frac{C}{\lambda}$, $\lambda \Rightarrow$ wavelength. Although the "group" velocity of light in a material medium is less than C, the velocity of a photon is always C, irrespective of the medium through which the light travels.[6]

The light emitting diode used for this work produced light with a wavelength of 900 nm, thus, the energy of one photon is:

$$E = \frac{hC}{\lambda} = \frac{[6.626\,(10)^{-34}\ \text{joule-second}]\,[2.998\,(10)^{8}\ \text{m/sec}]}{900\,(10)^{-9}\ \text{m}}$$

$E = 2.207\,(10)^{-19}$ joules, or

$$E = 2.207\,(10)^{-19}\ \text{joules}\left[\frac{6.242\,(10)^{18}\ \text{electron volts}}{\text{joule}}\right]$$

$E = 1.378$ electron volts.

APPENDIX B. CHANGE OF OPTICAL POWER IN DECIBELS

The change of optical power in decibels, dB, can be found by two methods. The methods are illustrated by using the results in Table 2 for 100/140/285 optical fiber.

1. Using the reference (original) and the reduced signal power:

$$dB = 10 \log \frac{P_{sig}}{P_{ref}} = 10 \log \frac{12.70\ nW}{28.05\ nW} = -3.44\ dB.$$

2. Using the percentage change in power, Δ_p:

$$dB = 10 \log \left(\frac{\Delta_p}{100} + 1 \right) = 10 \log \left(\frac{-54.72}{100} + 1 \right) = -3.44\ dB.$$

6 BROWN, E. B. *Modern Optics*. Reinhold Publishing Company, New York, New York, 1965, p. 13.

DISTRIBUTION LIST

No. of Copies	To
1	Office of the Under Secretary of Defense for Research and Engineering, The Pentagon, Washington, DC 20301
	Commander, U.S. Army Laboratory Command, 2800 Powder Mill Road, Adelphi, MD 20783-1145
1	ATTN: AMSLC-IM-TL
	Commander, Defense Technical Information Center, Cameron Station, Building 5, 5010 Duke Street, Alexandria, VA 22304-6145
2	ATTN: DTIC-FDAC
1	Metals and Ceramics Information Center, Battelle Columbus Laboratories, 505 King Avenue, Columbus, OH 43201
	Commander, Army Research Office, P.O. Box 12211, Research Triangle Park, NC 27709-2211
1	ATTN: Information Processing Office
	Commander, U.S. Army Materiel Command, 5001 Eisenhower Avenue, Alexandria, VA 22333
1	ATTN: AMCLD
	Commander, U.S. Army Materiel Systems Analysis Activity, Aberdeen Proving Ground, MD 21005
1	ATTN: AMXSY-MP, H. Cohen
	Commander, U.S. Army Electronics Research and Development Command, Fort Monmouth, NJ 07703
1	ATTN: AMDSD-L
1	AMDSD-E
	Commander, U.S. Army Missile Command, Redstone Scientific Information Center, Redstone Arsenal, AL 35898-5241
1	ATTN: AMSMI-RKP, J. Wright, Bldg. 7574
1	AMSMI-RD-CS-R/Doc
1	AMSMI-RLM
	Commander, U.S. Army Armament, Munitions and Chemical Command, Dover, NJ 07801
2	ATTN: Technical Library
1	AMDAR-LCA, Mr. Harry E. Pebly, Jr., PLASTEC, Director
	Commander, U.S. Army Natick Research, Development, and Engineering Center, Natick, MA 01760
1	ATTN: Technical Library
	Commander, U.S. Army Satellite Communications Agency, Fort Monmouth, NJ 07703
1	ATTN: Technical Document Center
	Commander, U.S. Army Tank-Automotive Command, Warren, MI 4397-5000
1	ATTN: AMSTA-ZSK
2	AMSTA-TSL, Technical Library
	Commander, White Sands Missile Range, NM 88002
1	ATTN: STEWS-WS-VT
	President, Airborne, Electronics and Special Warfare Board, Fort Bragg, NC 28307
1	ATTN: Library
	Director, U.S. Army Ballistic Research Laboratory, Aberdeen Proving Ground, MD 21005
1	ATTN: SLCBR-TSB-S (STINFO)
	Commander, Dugway Proving Ground, Dugway, UT 84022
1	ATTN: Technical Library, Technical Information Division
	Commander, Harry Diamond Laboratories, 2800 Powder Mill Road, Adelphi, MD 20783
1	ATTN: Technical Information Office
	Director, Benet Weapons Laboratory, LCWSL, USA AMCCOM, Watervliet, NY 12189
1	ATTN: AMSMC-LCB-TL
1	AMSMC-LCB-R
1	AMSMC-LCB-RM
1	AMSMC-LCB-RP
	Commander, U.S. Army Foreign Science and Technology Center, 220 7th Street, N.E., Charlottesville, VA 22901
1	ATTN: Military Tech

No. of Copies	To
	Commander, U.S. Army Aeromedical Research Unit, P.O. Box 577, Fort Rucker, AL 36360
1	ATTN: Technical Library
	Director, Eustis Directorate, U.S. Army Air Mobility Research and Development Laboratory, Fort Eustis, VA 23604-5577
1	ATTN: SAVDL-E-MOS (AVSCOM)
	U.S. Army Aviation Training Library, Fort Rucker, AL 36360
1	ATTN: Building 5906-5907
	Commander, U.S. Army Agency for Aviation Safety, Fort Rucker, AL 36362
1	ATTN: Technical Library
	Commander, USACDC Air Defense Agency, Fort Bliss, TX 79916
1	ATTN: Technical Library
	Commander, U.S. Army Engineer School, Fort Belvoir, VA 22060
1	ATTN: Library
	Commander, U.S. Army Engineer Waterways Experiment Station, P. O. Box 631, Vicksburg, MS 39180
1	ATTN: Research Center Library
	Commandant, U.S. Army Quartermaster School, Fort Lee, VA 23801
1	ATTN: Quartermaster School Library
	Naval Research Laboratory, Washington, DC 20375
1	ATTN: Code 5830
2	Dr. G. R. Yoder - Code 6384
	Chief of Naval Research, Arlington, VA 22217
1	ATTN: Code 471
1	Edward J. Morrissey, AFWAL/MLTE, Wright-Patterson Air Force, Base, OH 45433
	Commander, U.S. Air Force Wright Aeronautical Laboratories, Wright-Patterson Air Force Base, OH 45433
1	ATTN: AFWAL/MLC
1	AFWAL/MLLP, M. Forney, Jr.
1	AFWAL/MLBC, Mr. Stanley Schulman
	National Aeronautics and Space Administration, Marshall Space Flight Center, Huntsville, AL 35812
1	ATTN: R. J. Schwinghammer, EH01, Dir, M&P Lab
1	Mr. W. A. Wilson, EH41, Bldg. 4612
	U.S. Department of Commerce, National Institute of Standards and Technology, Gaithersburg, MD 20899
1	ATTN: Stephen M. Hsu, Chief, Ceramics Division, Institute for Materials Science and Engineering
1	Committee on Marine Structures, Marine Board, National Research Council, 2101 Constitution Ave., N.W., Washington, DC 20418
1	Librarian, Materials Sciences Corporation, Guynedd Plaza II, Bethlehem Pike, Spring House, PA 19477
1	The Charles Stark Draper Laboratory, 68 Albany Street, Cambridge, MA 02139
	Wyman-Gordon Company, Worcester, MA 01601
1	ATTN: Technical Library
	Lockheed-Georgia Company, 86 South Cobb Drive, Marietta, GA 30063
1	ATTN: Materials and Processes Engineering Dept. 71-11, Zone 54
	General Dynamics, Convair Aerospace Division, P.O. Box 748, Fort Worth, TX 76101
1	ATTN: Mfg. Engineering Technical Library
1	Mechanical Properties Data Center, Belfour Stulen Inc., 13917 W. Bay Shore Drive, Traverse City, MI 49684
1	Mr. R. J. Zentner, EAI Corporation, 626 Towne Center Drive, Suite 205, Joppatowne, MD 21085-4440
	Director, U.S. Army Materials Technology Laboratory, Watertown, MA 02172-0001
2	ATTN: SLCMT-TML
1	Author

U.S. Army Materials Technology Laboratory
Watertown, Massachusetts 02172-0001
THE QUANTITATIVE DEPENDENCE OF TRANSMISSIVITY ON FLEXURAL STRAIN FOR MULTIMODE OPTICAL FIBER - James A. Kidd, Jr.

Technical Report MTL TR 89-14, February 1989, 24 pp-illus-table, AMCMS Code No. 53970M6350

AD______________
UNCLASSIFIED
UNLIMITED DISTRIBUTION

Key Words

Optical fibers
Fiber optics
Attenuation

Four different multimode optical fibers were tested to obtain the following correlations: 1) signal power with bend radius, 2) strain with bend radius, and 3) signal power with strain. The data are presented numerically, graphically, and mathematically. Graded index multimode and step index multimode fibers are discussed. The mechanism for the attenuation of light in optical fiber as a result of macrobending is examined. Three of the tested fibers demonstrated a consistent relationship between flexural strain and light transmissivity and could potentially be inlaid within a curved composite material system for use as the principal component in a stress or strain transducer.

U.S. Army Materials Technology Laboratory
Watertown, Massachusetts 02172-0001
THE QUANTITATIVE DEPENDENCE OF TRANSMISSIVITY ON FLEXURAL STRAIN FOR MULTIMODE OPTICAL FIBER - James A. Kidd, Jr.

Technical Report MTL TR 89-14, February 1989, 24 pp-illus-table, AMCMS Code No. 53970M6350

AD______________
UNCLASSIFIED
UNLIMITED DISTRIBUTION

Key Words

Optical fibers
Fiber optics
Attenuation

Four different multimode optical fibers were tested to obtain the following correlations: 1) signal power with bend radius, 2) strain with bend radius, and 3) signal power with strain. The data are presented numerically, graphically, and mathematically. Graded index multimode and step index multimode fibers are discussed. The mechanism for the attenuation of light in optical fiber as a result of macrobending is examined. Three of the tested fibers demonstrated a consistent relationship between flexural strain and light transmissivity and could potentially be inlaid within a curved composite material system for use as the principal component in a stress or strain transducer.

U.S. Army Materials Technology Laboratory
Watertown, Massachusetts 02172-0001
THE QUANTITATIVE DEPENDENCE OF TRANSMISSIVITY ON FLEXURAL STRAIN FOR MULTIMODE OPTICAL FIBER - James A. Kidd, Jr.

Technical Report MTL TR 89-14, February 1989, 24 pp-illus-table, AMCMS Code No. 53970M6350

AD______________
UNCLASSIFIED
UNLIMITED DISTRIBUTION

Key Words

Optical fibers
Fiber optics
Attenuation

Four different multimode optical fibers were tested to obtain the following correlations: 1) signal power with bend radius, 2) strain with bend radius, and 3) signal power with strain. The data are presented numerically, graphically, and mathematically. Graded index multimode and step index multimode fibers are discussed. The mechanism for the attenuation of light in optical fiber as a result of macrobending is examined. Three of the tested fibers demonstrated a consistent relationship between flexural strain and light transmissivity and could potentially be inlaid within a curved composite material system for use as the principal component in a stress or strain transducer.

U.S. Army Materials Technology Laboratory
Watertown, Massachusetts 02172-0001
THE QUANTITATIVE DEPENDENCE OF TRANSMISSIVITY ON FLEXURAL STRAIN FOR MULTIMODE OPTICAL FIBER - James A. Kidd, Jr.

Technical Report MTL TR 89-14, February 1989, 24 pp-illus-table, AMCMS Code No. 53970M6350

AD______________
UNCLASSIFIED
UNLIMITED DISTRIBUTION

Key Words

Optical fibers
Fiber optics
Attenuation

Four different multimode optical fibers were tested to obtain the following correlations: 1) signal power with bend radius, 2) strain with bend radius, and 3) signal power with strain. The data are presented numerically, graphically, and mathematically. Graded index multimode and step index multimode fibers are discussed. The mechanism for the attenuation of light in optical fiber as a result of macrobending is examined. Three of the tested fibers demonstrated a consistent relationship between flexural strain and light transmissivity and could potentially be inlaid within a curved composite material system for use as the principal component in a stress or strain transducer.

END

6-89

DTIC